Quantification of singlet oxygen generation from photodynamic hydrogels

Craig, R. A., McCoy, C. P., De Baroid, A. T., Andrews, G. P., Gorman, S. P., & Jones, D. S. (2015). Quantification of singlet oxygen generation from photodynamic hydrogels. Reactive and Functional Polymers, 87, 1-6. DOI: 10.1016/j.reactfunctpolym.2014.11.009

Published in:
Reactive and Functional Polymers

Document Version:
Peer reviewed version

Queen's University Belfast - Research Portal:
Link to publication record in Queen's University Belfast Research Portal

Quantification of singlet oxygen generation from photodynamic hydrogels

Rebecca A. Craig, Colin P. McCoy*, Áine T. De Baróid, Gavin P. Andrews, Sean P. Gorman, David S. Jones

School of Pharmacy, Queen's University Belfast, Belfast, BT9 7BL, U.K.

*Corresponding author. Tel.: +44 28 9097 2081; fax: +44 28 9024 7794.

email address: c.mccoy@qub.ac.uk (C.P. McCoy)

Abstract

Recently, we described a series of novel porphyrin-impregnated hydrogels capable of producing microbicidal singlet oxygen ($^1O_2$) on photoactivation. Indirect assessment of the efficacy of $^1O_2$ production from such hydrogels has been previously described using microbiological techniques, but here we report a novel, direct method of quantification. Anthracene-9,10-dipropionic acid (ADPA) is known to irreversibly form an endoperoxide on reaction with $^1O_2$, causing photobleaching of its absorbance band at approximately 378 nm. Here, the reaction of this probe is exploited in a novel way to provide a simple, inexpensive, and convenient measurement of $^1O_2$ generation from the surface of porphyrin-incorporated photosensitising hydrogels, with the ability to account for effects due to hydrogel porosity. Ingress of the probe into the materials was observed, with rates of up to 3.83×10^3 s^{-1}. This varied by up to 200-fold with material composition and surface modification. Rates of $^1O_2$ generation in these porphyrin-incorporated hydrogels, after compensating for ADPA ingress, ranged from

$1.86x10^3 – 5.86x10^3$ s^{-1}. This work demonstrates a simple and straightforward method for direct $^1O_2$ quantification from porous materials, with general utility.

Keywords: porphyrin; hydrogel; singlet oxygen; quantification

1. Introduction

The high reactivity of photosensitiser-generated singlet oxygen ($^1O_2$) has led to its exploitation for photodynamic therapy and photodynamic antimicrobial chemotherapy, and it therefore plays an important role in a number of clinical and antimicrobial treatments and areas of research [1-3]. Recently, we have prepared photosensitiser-incorporated hydrogels for ocular applications [4]. On application of visible light to these hydrogels, $^1O_2$ is generated through the reaction of the excited state of the photosensitiser with molecular oxygen via what is often referred to as a type II pathway. This reaction is catalytic, with the photosensitiser unconsumed in the process. Additional reactive oxygen species such as superoxide anions and hydroxyl radicals may be generated via a type I pathway, but it is known that antioxidant enzymes in bacteria, which can protect against a number of reactive oxygen species, are ineffective against $^1O_2$ [5,6] (Kim, Wainwright). As it is widely accepted and has been experimentally determined that $^1O_2$ predominates in the mechanism of photosensitized cell death [7-9] (Ergaieg et al, Tavares et al, Bonnett), the quantification of $^1O_2$, particularly from porphyrin photosensitisers, is of great significance, and is becoming more necessary as the study and use of photosensitiser-incorporated systems grows.

The detection and quantification of $^1O_2$ from photocatalytic surfaces, however, remains in many ways problematic. To date, only indirect microbiological methods have been used, whereby the adherence of micro-organisms is characterised following irradiation. While this provides a useful assessment of the antimicrobial properties of the materials, it does not distinguish if these properties are due solely to $^1O_2$ generation, and as such cannot provide accurate or quantitative information regarding the rate of $^1O_2$ generation. A previously-reported procedure for the direct physical detection of $^1O_2$ from hydrogels involves measurement of the near-infrared luminescence of $^1O_2$ at 1270 nm [10]. Due to the short lifetime of $^1O_2$ in aqueous solution, its poor solubility, and the low quantum yield of the transition back to ground state, detection by this method is challenging. We previously described a method for directly measuring $^1O_2$ generation from hydrogel surfaces, involving a liquid-nitrogen-cooled Indium Gallium Arsenide detector [11], which is complex, expensive, and custom-designed, due to the insensitivity of most conventional photomultipliers at the wavelength of $^1O_2$ fluorescence emission. Furthermore, data deconvolution due to competing processes is complex. It is therefore desirable to find an inexpensive, rapid, and effective alternative means of testing in aqueous media to provide a general method of quantification of $^1O_2$ generation from materials surfaces, including porous materials such as hydrogels. Given the potentially numerous biological applications of these anti-infective materials, a method which is readily applicable to aqueous systems is particularly relevant.

A number of chemical methods to detect $^1O_2$ have been described, involving the use of a chemical probe that reacts with $^1O_2$ to form an endoperoxide. Generally, the probe itself can be spectroscopically characterised in terms of sensitive UV-visible

absorbance or fluorescence emission, but the endoperoxide does not possess absorbance or emission in the same wavelength range as the parent molecule, as its formation breaks an extended π-system found in the parent molecule. The ability to monitor this reaction spectrophotometrically allows sensitive and convenient measurement. Some compounds used include 9,10-dimethyl anthracene [12], 2,5-dimethylfuran [13], anthracene-9,10-diyldiethyl disulfate (EAS), bis-9,10-anthracene-(4-trimethyl-phenylammonium)dichloride (BPAA) [14], anthracene-9,10-divinylsulfonate (AVS) [15], anthracene-9,10-bisethanesulfonic acid (AES) [15,16], and anthracene-9,10-dipropionic acid (ADPA) [17]. EAS, AVS, and AES are anionic and therefore may bind with cationic photosensitisers. As TMPyP is tetracationic, they are unsuitable for this study. 2,5-dimethylfuran is only soluble in lipid matrices, also rendering it unsuitable for use in the aqueous systems in which biologically-active polymers are used, and BPAA is cationic which may lead to interaction between it and any unbound anionic methacrylic acid groups at the polymer surface. Singlet Oxygen Sensor Green (SOSG), a commercially available sensor, has also been widely used but it is associated with a number of drawbacks including photodecomposition, intersystem crossing, and $^1O_2$ generation, thus interfering with quantification of photosensitiser-generated $^1O_2$ [17].

The use of ADPA in the detection of $^1O_2$ was first described by Lindig *et al*. [18]. It has since been employed to assess $^1O_2$ generation by various photosensitiser systems including methylene blue-containing polyacrylamide and silica nanoparticles [19], butadiyne-bridged bisporphyrin for photodynamic therapy (PDT) [20], and meta-tetra(hydroxyphenyl)-chlorin containing silica nanoparticles for PDT [21], and a polymer-based porphyrin system [22]. It has also been used to quantify $^1O_2$ generation

from porous hydrogel particles, but without taking into account ingress into the hydrogel [23]. ADPA ingress into the bulk material is the major hurdle to be overcome in quantification of $^1O_2$ generation from porous materials, and is addressed in the present study as such as method is currently absent from the literature.

ADPA reacts very rapidly and irreversibly with $^1O_2$ to produce an endoperoxide, resulting in bleaching of the absorbance maximum of ADPA at approximately 378 nm [18,22] (Scheme 1). The endoperoxide formed is thermally stable at room temperature [23]. It is a useful method of quantification as, even when $^1O_2$ generation rates are low, the concentration of endoperoxide produced remains proportional to the cumulative amount of $^1O_2$ generated [12]. In addition, it has a high rate constant for reaction with $^1O_2$ [18,24] and high water solubility, which allows testing in aqueous media, and in systems with biological applications.

This reaction is demonstrated here to provide a quantitative measure of the role of $^1O_2$ generation at the surface of a series of porphyrin-incorporated hydrogels, and therefore provide an indication of their bactericidal activity. This method is distinctive from previously reported uses of ADPA in that it can account for ingress of ADPA into the materials under evaluation. This is the first use, to our knowledge, of this probe for detection of $^1O_2$ generation from porous bulk hydrogels.

2. Materials and Methods

2.1 Materials

Anthracene-9,10-dipropionic acid disodium salt (ADPA) was obtained from Chemodex (St. Gallen, Switzerland). Tetrakis(4-N-methylpyridyl)porphyrin (TMPyP), 2-hydroxyethyl methacrylate 97% (HEMA), methyl methacrylate 99% (MMA), methacrylic acid 99% (MAA), ethylene glycol dimethacrylate 98% (EGDMA), and benzoyl peroxide 70% (BPO) were obtained from Aldrich (U.K.) and used as supplied.

2.2. Preparation of solutions

ADPA solutions were prepared in 20:80 (v/v) methanol: deionised water. All UV-visible absorption measurements were obtained using a PerkinElmer Lambda 650 UV-visible spectrophotometer with a tungsten-halogen lamp, and viewed using UVWinLab software (PerkinElmer, USA).

For solution studies, TMPyP, at various concentrations, and ADPA were dissolved in 20:80 (v/v) methanol: deionised water, with a final ADPA concentration of 5.22×10^{-5} mol/dm^3. A control solution of ADPA (5.22×10^{-5} mol/dm^3) in 20:80 (v/v) methanol: deionised water, containing no TMPyP was also tested. Solutions were exposed to white light (8.91 mW/cm^2) generated from 25 W halogen lights (Halolux Ceram, Osram, Germany), at a fixed distance of 11 cm for time periods ranging from 5-20 minutes, with the use of a fan to maintain temperature at 27°C, or maintained in dark conditions. Absorption spectra were recorded between 320-550 nm, allowing visualisation of the main absorption peaks of ADPA, and the Soret band of TMPyP.

To quantify the $^1O_2$ generated by TMPyP on irradiation, the reactions occurring in solution require consideration. Scheme 2 describes the processes that occur when ADPA and TMPyP are irradiated together in solution (modified from [19,21]):

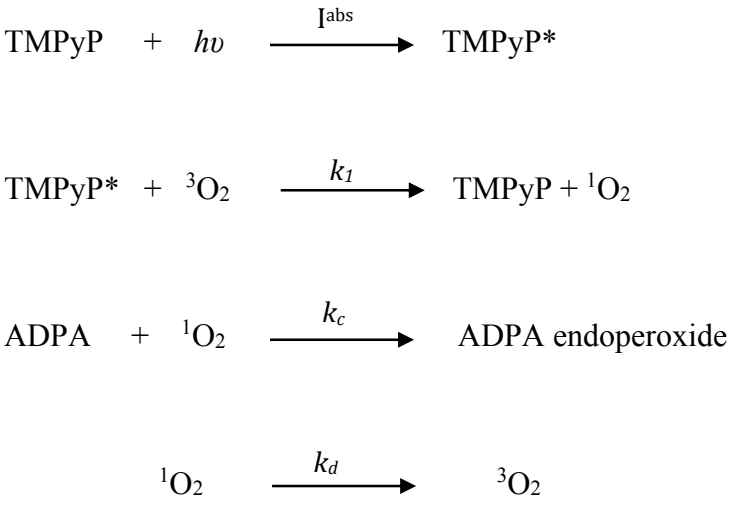

Scheme 2. The series of reactions that occur in solution, resulting in photobleaching of ADPA. I^{abs} indicates intensity of absorbance, k_1, k_c and k_d are rate constants.

TMPyP represents TMPyP in the ground state either in solution or electrostatically bound to the polymer surface. On application of light it is excited to TMPyP* at a rate that equals the intensity of light absorbed, I^{abs}. TMPyP* can then transfer energy to ground state oxygen, $^3O_2$, causing its excitation to singlet oxygen, $^1O_2$. The rate constant of TMPyP* quenching by $^3O_2$ is k_1. The generated $^1O_2$ can then react with ADPA, irreversibly forming ADPA endoperoxide with a rate constant k_c. $^1O_2$ can also decay to the ground state by transferring energy to the solvent or other species in the solution, with a rate constant k_d.

The loss of ADPA, and formation of an endoperoxide, on reaction with $^1O_2$ can be described by Equation 1.

$$-\frac{d[ADPA]}{dt} = k_c[ADPA][^1O_2] \qquad \text{Equation 1}$$

Assuming that $k_d >> k_c$, makes the rate equation for $^1O_2$ independent of [ADPA], so that it is not changed over the period of irradiation. The loss of ADPA, then, follows first order kinetics (Equation 2).

$$\frac{[ADPA]}{[ADPA]_0} = e^{(-kt)} \qquad \text{Equation 2}$$

In Equation 2, [ADPA] and $[ADPA]_0$ are the ADPA concentrations at time t, and time 0 respectively; $[^1O_2]_0$ is the $^1O_2$ concentration before significant loss in other potential reaction steps, and the rate constant k is equal to $(\Phi^{^1O_2} I^{abs} k_c)/k_d$.

Due to the proportionality between ADPA concentration and UV-visible absorbance, a plot of ln $(A)/(A_0)$ *vs* t allows the rate constant (k) to be obtained from the gradient, where A is the absorbance at time t, and A_0 is the absorbance at time 0.

2.3. Preparation of hydrogels for analysis

Acrylate hydrogels were fabricated as previously described [4] *via* free radical-initiated polymerisation of the co-monomers. Tables 1 and 2 describe the relative quantities of co-monomers in each hydrogel copolymer, and the corresponding sample code for each.

Table 1. Hydrogel copolymers prepared by varying MMA content at the expense of HEMA, whilst maintaining MAA at 10%. Denoted hereafter as MMA series, with sample codes as listed. Percentages reflect the percentage composition of co-monomers in the fabricated material by weight.

MMA	MAA	HEMA	Sample code
0	10	90	0MMA
5	10	85	5MMA
10	10	80	10MMA
15	10	75	15MMA

Table 2. Hydrogel copolymers prepared by varying MAA content at the expense of HEMA, whilst maintaining MMA at 5%. Denoted hereafter as MAA series, with sample codes as listed. Percentages reflect the percentage composition of co-monomers in the fabricated material by weight.

MAA	MMA	HEMA	Sample code
0	5	95	0MAA
10	5	85	10MAA
20	5	75	20MAA
30	5	65	30MAA

2.4. Assessment of $^1O_2$ production from porphyrin-incorporated and untreated hydrogels

Porphyrin was incorporated into hydrogel samples (20 x 5 mm) 24 hours prior to testing by dipping into a 10 mg/100 ml TMPyP solution (phosphate-buffered saline (PBS), pH 7.4) for 2 minutes, followed by rinsing with and soaking in deionised water. Corresponding untreated samples were prepared, without exposure to TMPyP. Representative treated and untreated samples are shown in Figure 1.

Porphyrin-incorporated and untreated hydrogel samples were placed in polystyrene cuvettes (1 cm pathlength) with 3 ml ADPA solution (concentration 2.38 x 10^{-5} mol/dm^3), made as described, and subjected either to white light irradiation (8.91 mW/cm^2) as described at a fixed distance of 11 cm, or to dark conditions, for 20 minute periods with collection of the UV absorbance spectrum following each irradiation. Data was collected over 140 minutes. The gradient of the resultant first order plots was used to calculate the rate of ADPA photobleaching, and thus quantify the $^1O_2$ generation by the hydrogels, according to Equation 2. The rate of decrease in absorbance in materials treated in the same way but kept in the dark was used to correct for ingress of ADPA into each material.

3. Results and Discussion

The purpose of this study was to establish a simple and robust method for quantification of $^1O_2$ generation from photosensitiser-incorporated hydrogels, thus providing an alternative to the currently available, and more complex, direct physical methods.

ADPA has previously been used in a number of studies for the detection of $^1O_2$, but this is the first published study for its use in quantification of $^1O_2$ from porous bulk hydrogels.

3.1. Solution studies

Characterisation of ADPA, and of the $^1O_2$ generation of TMPyP, was performed in solution and monitored with UV-visible spectroscopy. Four vibrational peaks were observed in the UV-visible absorption spectrum of ADPA at 399, 378, 359, and 342 nm (Figure 2), corresponding to reported literature values [20]. No shift in the main ADPA peaks was observed when in solution with TMPyP, (Figure 3), indicating no molecular interaction between the two compounds at the concentrations used. With each successive irradiation of the ADPA/TMPyP solution, decreases in the ADPA absorption peaks are seen, showing an approximate decrease of 40% over 80 min.

These data confirm the generation of $^1O_2$ on irradiation, and its reaction with ADPA. When ADPA solution was irradiated in the absence of TMPyP, no decrease in absorbance occurred, highlighting the necessity of a $^1O_2$ generator to cause ADPA photobleaching.

The rate constant for quenching of ADPA by TMPyP-generated $^1O_2$ in aqueous solution was calculated using Equation 2. Due to the proportionality between ADPA concentration and UV absorbance, this was plotted using the calculated absorbance values as $\ln(A)/(A_0)$ *vs* t where A is the absorbance at time t, and A_0 is the absorbance at time 0 (Figure 4).

The rate constant, *k*, was obtained from the gradient of the first order plot. The linear rate of quenching (0.0062 s^{-1}) of ADPA by TMPyP-generated $^1O_2$ confirms the utility of ADPA in monitoring of $^1O_2$ generation from TMPyP, and the suitability of ADPA as a chemical probe for $^1O_2$ from TMPyP. The necessity for the presence of both light and photosensitiser for $^1O_2$ generation is also confirmed.

3.2. Polymer studies

Having established an absence of interaction between TMPyP and ADPA, and the ability of photogenerated $^1O_2$ from TMPyP to cause ADPA photobleaching, the study was applied to the fabricated hydrogel samples. As with the solution studies, linear first order plots were obtained following irradiation of hydrogel samples (Figure 5).

ADPA absorbance decreases were noted with untreated hydrogel samples, both when irradiated and kept in the dark, and with treated samples kept in dark conditions. This is attributed to uptake of ADPA by the porous hydrogels. The rate constant for ADPA uptake by each material was calculated from the gradient of the first order plots, and is shown in Tables 3 and 4.

Table 3. Rate of uptake of ADPA by each material in the MAA series following 140 minutes contact with the materials. Values for untreated materials are calculated as an

average of rate constants of uptake when in light and dark conditions; values for porphyrin-incorporated materials are obtained from the sample kept in the dark

	Rate of ADPA uptake (s^{-1})	
	Untreated material	**Porphyrin-incorporated material**
0MAA	$1.3 \times 10^{-3} \pm 2.84 \times 10^{-4}$	$3.80 \times 10^{-4} \pm 4.47 \times 10^{-5}$
10MAA	$8.0 \times 10^{-4} \pm 7.07 \times 10^{-5}$	$1.24 \times 10^{-5} \pm 7.67 \pm 10^{-6}$
20MAA	$5.54 \times 10^{-4} \pm 7.07 \times 10^{-5}$	$-7.80 \times 10^{-5} \pm 1.64 \times 10^{-5}$
30MAA	$5.50 \times 10^{-4} \pm 2.12 \times 10^{-4}$	$1.40 \times 10^{-4} \pm 5.48 \times 10^{-5}$

Table 4. Rate of uptake of ADPA by each material in the MMA series following 140 minutes contact with the materials. Values for untreated materials are calculated as an average of rate constants of uptake when in light and dark conditions; values for porphyrin-incorporated materials are obtained from the sample kept in the dark

	Rate of ADPA uptake (s^{-1})	
	Untreated material	**Porphyrin-incorporated material**
0MMA	$2.0 \times 10^{-3} \pm 1.41 \times 10^{-4}$	$2.40 \times 10^{-5} \pm 1.79 \times 10^{-5}$
5MMA	$9.01 \times 10^{-4} \pm 8.03 \times 10^{-5}$	$1.24 \times 10^{-5} \pm 7.69 \pm 10^{-6}$
10MMA	$3.83 \times 10^{-3} \pm 1.41 \times 10^{-4}$	$8.80 \times 10^{-6} \pm 7.42 \times 10^{-6}$
15MMA	$9.12 \times 10^{-4} \pm 2.84 \times 10^{-4}$	$2.60 \times 10^{-4} \pm 4.48 \times 10^{-5}$

Untreated hydrogel samples displayed similar uptake behaviour in both light and dark conditions, and this differed from that seen with porphyrin-incorporated samples by approximately 10-200 fold. Due to this differing uptake behaviour when in ADPA

solution, for each set of experiments the sample tested in the dark acted as a control for the corresponding irradiated sample. Using Equation 2, the rate constant, *k*, of $^1O_2$ generation, or of ADPA uptake, was calculated for each hydrogel. ADPA uptake into the irradiated porphyrin-incorporated materials was accounted for by subtraction of the rate of ADPA uptake into porphyrin-incorporated samples in the dark from the pseudo rate constant of the corresponding materials in the light. The resultant corrected first order rate constant, *k*, is proportional to the $^1O_2$ generation by each material. The rate constants for each material, corrected for ADPA uptake, are shown in Table 5.

Table 5. Rate constants of photobleaching for each irradiated porphyrin-incorporated material after correction for ADPA uptake by subtraction of the rate constant from porphyrin-incorporated materials kept in the dark.

	Rate constant, k (s^{-1})
0MAA	$4.64 \times 10^{-3} \pm 1.94 \times 10^{-4}$
10MAA	$3.09 \times 10^{-3} \pm 1.48 \times 10^{-4}$
20MAA	$3.48 \times 10^{-3} \pm 1.14 \times 10^{-4}$
30MAA	$5.76 \times 10^{-3} \pm 4.28 \times 10^{-4}$
0MMA	$3.08 \times 10^{-3} \pm 1.22 \times 10^{-4}$
5MMA	$3.09 \times 10^{-3} \pm 1.48 \times 10^{-4}$
10MMA	$1.87 \times 10^{-3} \pm 3.06 \times 10^{-4}$
15MMA	$6.34 \times 10^{-3} \pm 4.09 \times 10^{-4}$

The rate of $^1O_2$ generation from the hydrogel samples is first order, in agreement with $^1O_2$ generation kinetics commonly seen from other photosensitisers probed with ADPA, when either in solution or substrate-bound [19,20,23]. Hydrogel porosity, as anticipated, required consideration in the calculation of rate constants, with decreases in ADPA absorbance maximum at 378 nm being observed on irradiation of untreated

hydrogel samples. These decreases are attributed to ingress of ADPA (MW 366 g/mol) into the hydrogels, as the solution studies demonstrated that ADPA photobleaching does not occur in the absence of $^1O_2$. The rates of ADPA absorbance decrease at 378 nm were comparable for untreated hydrogels of the same composition, regardless of light conditions, thus supporting the attribution to ADPA uptake by the materials, and dismissing any possibility of decreases due to reaction with surface-localised TMPyP. When porphyrin-incorporated samples were tested in the dark, however, a much smaller or negligible ADPA ingress into the materials was noted in comparison to untreated samples, with the exception of those containing the smallest proportions of MAA (0MAA and 15MMA). The likely reason for the observed differences between treated and untreated hydrogels is the formation of a more dense surface layer on the surface of TMPyP-incorporated hydrogels, which reduces ingress of ADPA. TMPyP is known to be highly surface localised on hydrogels of this type [4]. In the case of low MAA content, the reduced availability of electrostatic binding sites decreases the density of TMPyP on the surface, therefore allowing a greater uptake of ADPA than the other materials studied. Additionally, in the presence of anionic MAA at the surface of the materials, the cationic TMPyP can neutralise surface charges, reducing the effect of charge repulsion between chains and allowing the polymer structure to relax, making it less porous. In the absence of MAA, impregnation with TMPyP renders the surface cationic, imposing more strain upon the polymer chains, as a result of charge repulsion, leading to an increase in polymer porosity. This accounts for the large uptake of ADPA observed in 0MAA in comparison with polymers containing MAA, and increased uptake in 15MMA compared with polymers containing more MAA.

As a result, uptake kinetics were therefore characterised separately for the porphyrin-incorporated and untreated hydrogels. The differences in uptake kinetics of approximately 10 to 200-fold, upon porphyrin-incorporation, and of approximately 10 to 70-fold upon change of hydrogel composition, highlight the degree with which ADPA uptake into bulk hydrogels can be altered with composition and surface modification. The rate of uptake is first order in all tested hydrogel samples, allowing simple subtraction from the rate of change of ADPA absorbance from the irradiated porphyrin-incorporated sample. This is, therefore, a generally applicable method for quantification of $^1O_2$ generation from hydrogels of any composition, provided that uptake behaviour is characterised and accounted for.

No correlation was observed between the rate of $^1O_2$ generation and material composition, as the TMPyP loading at the surface, rather than the material itself, is the primary determinant of $^1O_2$ concentration reaching the solution phase. The rate constants of $^1O_2$ generation from the studied materials are favourable when compared with the highest of those achieved with a published study involving the measurement of $^1O_2$ from porphyrin-polymer complexes, also using ADPA as a probe. The published values ranged from approximately 4×10^{-4} - 3×10^{-3} s^{-1} [22], whereas the values in the present study range between 1.89×10^{-3} - 5.86×10^{-3} s^{-1}, demonstrating the high efficiency of $^1O_2$ generation from these hydrogels on light application. Such a high efficiency is of pertinence given the predominant role of $^1O_2$ in TMPyP-mediated bacterial cell death [8].

4. Conclusions

Exploitation of ADPA photobleaching has been shown for the first time to provide a simple, inexpensive, and convenient method for measuring the rate of $^1O_2$ generation from the surface of porous porphyrin-incorporated bulk hydrogels in aqueous media, provided compensation is made for ADPA uptake by the materials. Quantification of $^1O_2$ generation from the present materials demonstrates rates of up to 5.86 x 10^3 s^{-1}, showing good efficiency. The uptake of ADPA can vary depending on the material composition and presence or absence of surface-localised photosensitiser. The method described is generally applicable to porous polymeric materials when uptake behaviour is characterised to ensure appropriate correction for ADPA uptake. Correction for uptake is straightforward, and the use of ADPA in the quantification of $^1O_2$ from porphyrin-incorporated hydrogels offers a number of advantages over the cumbersome direct physical methods that have been previously attempted for similar hydrogels. The method can, additionally, be generalised to materials which generate $^1O_2$ at their surface.

Acknowledgements

This work was funded by a grant from the Department for Employment and Learning, Northern Ireland, who played no role in the design of the study, data collection and analysis, preparation of the manuscript or in the decision to publish the findings.

References

[1] de Oliveira RR, Schwartz-Filho HO, Novaes AB, Jr., Taba M, Jr. Antimicrobial photodynamic therapy in the non-surgical treatment of aggressive periodontits: A preliminary randomized controlled clinical study. J Periodontol 78 (2007) 965-973.

[2] Jang MS, Doh KS, Kang JS, Jeon YS, Suh KS, Kim ST. A comparative split-face study of photodynamic therapy with indocyanine green and indole-3-acetic acid for the treatment of acne vulgaris. Br J Dermatol 165 (2011) 1095-1100.

[3] Brown SB, Brown EA, Walker I. The present and future role of photodynamic therapy in cancer treatment. 5 (2004) 497-508.

[4] McCoy CP, Craig RA, McGlinchey SM, Carson L, Jones DS, Gorman SP. Surface localisation of photosensitisers on intraocular lens biomaterials for prevention of infectious endophthalmitis and retinal protection. Biomaterials 33 (2012) 7952-7958.

[5] Kim SY, Kwon OJ, Park JW. Inactication of catalase and superoxide dismutase by singlet oxygen derived from photoactivated dye. Biochimie 83 (2001) 437-444.

[6] Wainwright M, Crossley KB. Photosensitising agents – circumventing resistance and breaking down biofilms: a review. Int Biodeter Biodegr 53 (2004) 119-126.

[7] Ergaieg K, Chevanne M, Cillard J, Seux R. Involvement of both type I and type II mechanisms in Gram-positive and Gram-negative bacteria photosensitization by a *meso*-substituted cationic porphyrin. Sol Energy 82 (2008) 1107-1117.

[8] Tavares A, Dias SR, Carvalho CM, Faustino MA, Tomé JP, Neves MG, Tomé AC, Cavalerio JA, Cunha Å, Gomes NC, Alves E, Almeida A. Mechanisms of photodynamic inactivation of a Gram-negative recombinant bioluminescent bacterium by cationic porphyrins. Photochem Photobiol Sci (2011) 1659-1669.

[9] Bonnett R. Photosensitizers of the porphyrin and phthalocyanine series for photodynamic therapy. Chem Soc Rev (1995) 19-33.

[10] Wu H, Song Q, Ran G, Lu X, Xu B. Recent developments in the detection of singlet oxygen with molecular spectroscopic methods. Trac-Trends Anal Chem 30 (2011) 133-141.

[11] Brady C, Bell SEJ, Parsons C, Gorman SP, Jones DS, McCoy CP. Novel Porphyrin-Incorporated Hydrogels for Photoactive Intraocular Lens Biomaterials. J Phys Chem B 111 (2007) 527-534.

[7] Cao Y, Koo Y, Koo S, Kopelman R. Ratiometric singlet oxygen nano-optodes and their use for monitoring photodynamic therapy nanoplatforms. Photochem Photobiol 81 (2005) 1489-1498.

[8] Becerra M, Sarmiento M, Paez P, Arguello G, Albesa I. Light effect and reactive oxygen species in the action of ciprofloxacin on *Staphylococcus aureus*. J Photochem Photobiol B 76 (2004) 13-18.

[9] Nardello V, Aubry J. Synthesis and properties of a new cationic water-soluble trap of singlet molecular oxygen. Tetrahedron Lett 38 (1997) 7361-7364.

[10] Nardello V, Aubry J, Johnston P, Bulduk I, de Vries A, Alsters P. Facile preparation of the water-soluble singlet oxygen traps anthracene-9,10-divinylsulfonate (AVS) and anthracene-9,10-diethylsulfonate (AES) via a heck reaction with vinylsulfonate. Synlett 17 (2005) 2667-2669.

[11] Botsivali M, Evans D. New trap for singlet oxygen in aqueous solution. J Chem Soc -Chem Commun 24 (1979) 1114-1116.

[12] Kim S, Fujitsuka M, Majima T. Photochemistry of Singlet Oxygen Sensor Green. J Phys Chem B 117 (2013) 13985-13992

[13] Lindig B, Rodgers M, Schapp A. Determination of the lifetime of singlet oxygen in D2O using 9,10-anthracenedipropionic acid, a water-soluble probe. J Am Chem Soc 102 (1980) 5590-5593.

[14] Tang W, Xu H, Kopelman R, Philbert M. Photodynamic characterization and in vitro application of methylene blue-containing nanoparticle platforms. Photochem Photobiol 81 (2005) 242-249.

[15] Dy J, Ogawa K, Satake A, Ishizumi A, Kobuke Y. Water-soluble self-assembled butadiyne-bridged bisporphyrin: A potential two-photon-absorbing photosensitizer for photodynamic therapy. 13 (2007) 3491-3500.

[16] Yan F, Kopelman R. The embedding of meta-tetra(hydroxyphenyl)-chlorin into silica nanoparticle platforms for photodynamic therapy and their singlet oxygen production and pH-dependent optical properties. Photochem Photobiol 78 (2003) 587-591.

[17] Xing C, Xu Q, Tang H, Liu L, Wang S. Conjugated polymer/porphyrin complexes for efficient energy transfer and improving light-activated antibacterial activity. J Am Chem Soc 131 (2009) 13117-13124.

[18] Moreno M, Monson E, Reddy R, Rehemtulla A, Ross B, Philbert M. Production of singlet oxygen by Ru(dpp(SO3)(2))(3) incorporated in polyacrylamide PEBBLES. Sensors Actuators B-Chemical 90 (2003) 82-89.

[19] Lindig B, Rodgers M. Rate parameters for the quenching of singlet oxygen by water-soluble and lipid-soluble substrates in aqueous and micellar systems. Photochem Photobiol 33 (1981) 627-634.

Figure captions

Figure 1. Representative untreated (left) and porphyrin-incorporated (right) hydrogel samples.

Figure 2. Overlaid UV-visible absorbance spectra of an ADPA solution (2.28 x 10^{-5} mol/dm^3), and a TMPyP solution (10 mg/100 ml).

Figure 3. Overlaid UV-visible absorbance spectra of ADPA: TMPyP 1 µg/ml (9:1) solution irradiated for 80 minutes. Time points measured are 0, 10, 20, 40, 60, and 80 minutes. Arrows represent the direction of change in absorbance with time.

Figure 4. First order plot for irradiation of a 9:1 ADPA:TMPyP solution, using data from the ADPA peak maximum at 378 nm.

Figure 5. Representative first order plots of (a) untreated 0MAA hydrogel and (b) porphyrin-incorporated 0MAA hydrogel following exposure to white light or dark conditions over a 140 minute period, with measurement at 20 minute intervals. Data are shown as mean ± SD.

Table captions

Table 1. Hydrogel copolymers prepared by varying MMA content at the expense of HEMA, whilst maintaining MAA at 10%. Denoted hereafter as MMA series, with sample codes as listed. Percentages reflect the percentage composition of co-monomers in the fabricated material by weight.

Table 2. Hydrogel copolymers prepared by varying MAA content at the expense of HEMA, whilst maintaining MMA at 5%. Denoted hereafter as MAA series, with sample codes as listed. Percentages reflect the percentage composition of co-monomers in the fabricated material by weight.

Table 3. Rate of uptake of ADPA by each material in the MAA series following 140 minutes contact with the materials. Values for untreated materials are calculated as an average of rate constants of uptake when in light and dark conditions; values for porphyrin-incorporated materials are obtained from the sample kept in the dark

Table 4. Rate of uptake of ADPA by each material in the MMA series following 140 minutes contact with the materials. Values for untreated materials are calculated as an average of rate constants of uptake when in light and dark conditions; values for porphyrin-incorporated materials are obtained from the sample kept in the dark

Table 5. Rate constants of photobleaching for each irradiated porphyrin-incorporated material after correction for ADPA uptake by subtraction of the rate constant from porphyrin-incorporated materials kept in the dark.

Scheme captions

Scheme 1. The conversion of ADPA to an endoperoxide on reaction with $^1O_2$.

Scheme 2. The series of reactions that occur in solution, resulting in photobleaching of ADPA. I^{abs} indicates intensity of absorbance, k_1, k_c and k_d are rate constants.

Schemes and Figures

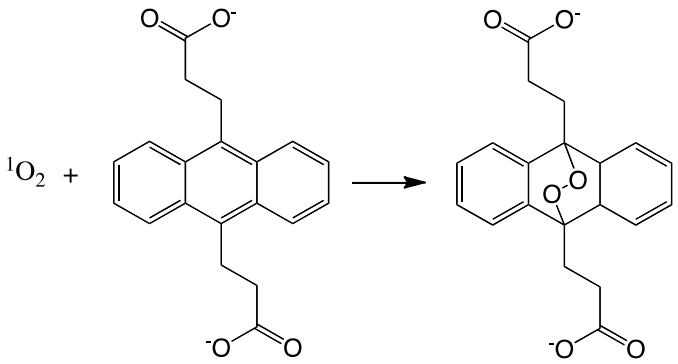

Scheme 1. The conversion of ADPA to an endoperoxide on reaction with $^1O_2$.

$$TMPyP + h\upsilon \xrightarrow{I^{abs}} TMPyP^*$$

$$TMPyP^* + {}^3O_2 \xrightarrow{k_1} TMPyP + {}^1O_2$$

$$ADPA + {}^1O_2 \xrightarrow{k_c} ADPA\ endoperoxide$$

$$^1O_2 \xrightarrow{k_d} {}^3O_2$$

Scheme 2. The series of reactions that occur in solution, resulting in photobleaching of ADPA. I^{abs} indicates intensity of absorbance, k_1, k_c and k_d are rate constants.

Figure 1. Representative untreated (left) and porphyrin-incorporated (right) hydrogel samples.

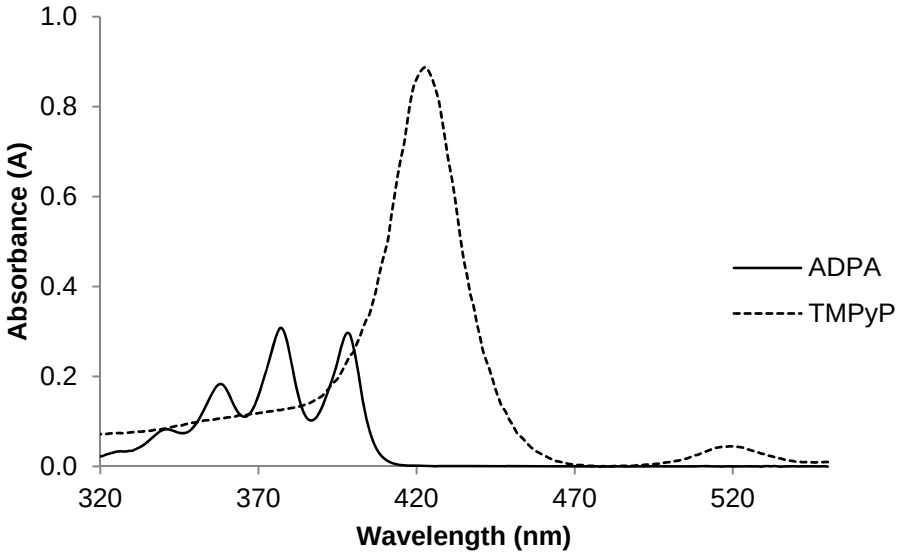

Figure 2. Overlaid UV-visible absorbance spectra of an ADPA solution (2.28 x 10^{-5} mol/dm^3), and a TMPyP solution (10 mg/100 ml).

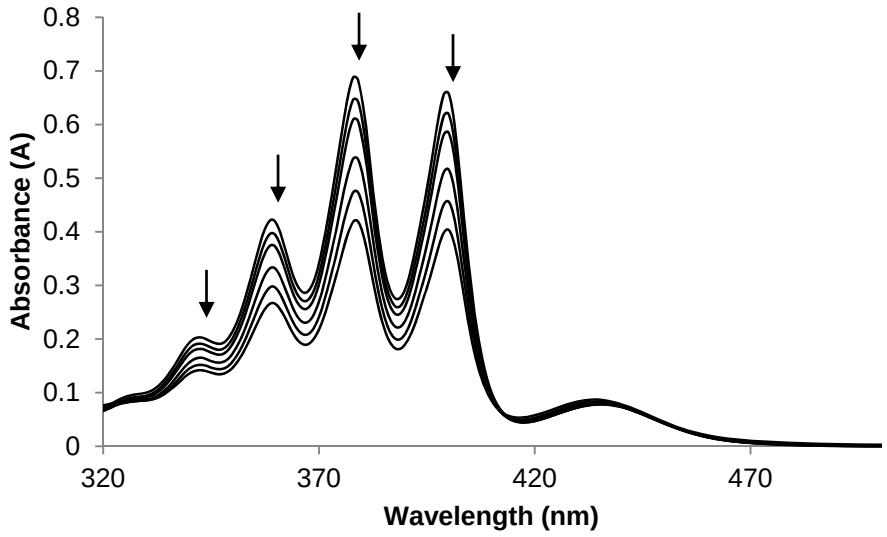

Figure 3. Overlaid UV-visible absorbance spectra of ADPA: TMPyP 1 µg/ml (9:1) solution irradiated for 80 minutes. Time points measured are 0, 10, 20, 40, 60, and 80 minutes. Arrows represent the direction of change in absorbance with time.

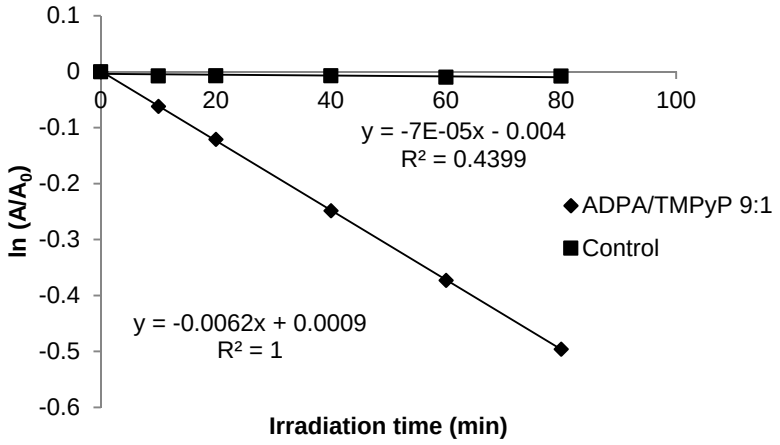

Figure 4. First order plot for irradiation of a 9:1 ADPA:TMPyP solution, using data from the ADPA peak maximum at 378 nm.

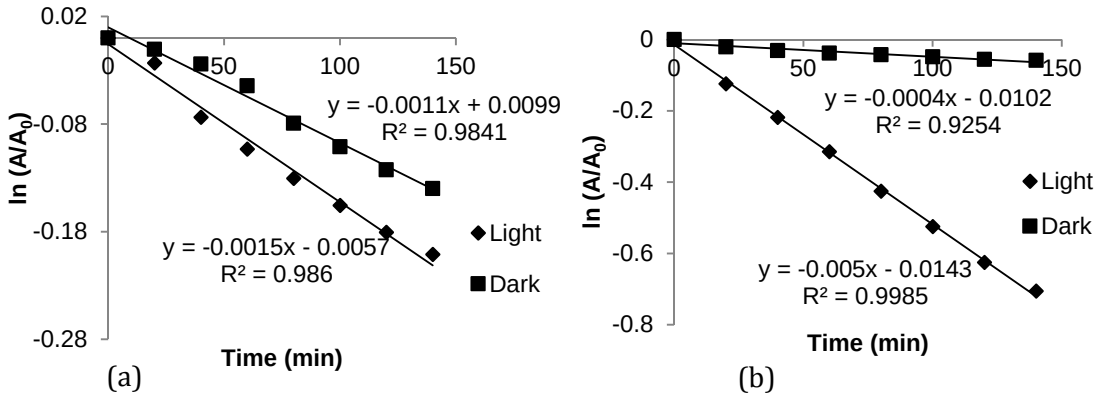

Figure 5. Representative first order plots of (a) untreated 0MAA hydrogel and (b) porphyrin-incorporated 0MAA hydrogel following exposure to white light or dark conditions over a 140 minute period, with measurement at 20 minute intervals. Data are shown as mean ± SD.

Tables

Table 1. Hydrogel copolymers prepared by varying MMA content at the expense of HEMA, whilst maintaining MAA at 10%. Denoted hereafter as MMA series, with sample codes as listed. Percentages reflect the percentage composition of co-monomers in the fabricated material by weight.

MMA	MAA	HEMA	Sample code
0	10	90	0MMA
5	10	85	5MMA
10	10	80	10MMA
15	10	75	15MMA

Table 2. Hydrogel copolymers prepared by varying MAA content at the expense of HEMA, whilst maintaining MMA at 5%. Denoted hereafter as MAA series, with sample codes as listed. Percentages reflect the percentage composition of co-monomers in the fabricated material by weight.

MAA	MMA	HEMA	Sample code
0	5	95	0MAA
10	5	85	10MAA
20	5	75	20MAA
30	5	65	30MAA

Table 3. Rate of uptake of ADPA by each material in the MAA series following 140 minutes contact with the materials. Values for untreated materials are calculated as an average of rate constants of uptake when in light and dark conditions; values for porphyrin-incorporated materials are obtained from the sample kept in the dark

	Rate of ADPA uptake (s^{-1})	
	Untreated material	**Porphyrin-incorporated material**
0MAA	$1.3 \times 10^{-3} \pm 2.84 \times 10^{-4}$	$3.80 \times 10^{-4} \pm 4.47 \times 10^{-5}$
10MAA	$8.0 \times 10^{-4} \pm 7.07 \times 10^{-5}$	$1.24 \times 10^{-5} \pm 7.67 \pm 10^{-6}$
20MAA	$5.54 \times 10^{-4} \pm 7.07 \times 10^{-5}$	$-7.80 \times 10^{-5} \pm 1.64 \times 10^{-5}$
30MAA	$5.50 \times 10^{-4} \pm 2.12 \times 10^{-4}$	$1.40 \times 10^{-4} \pm 5.48 \times 10^{-5}$

Table 4. Rate of uptake of ADPA by each material in the MMA series following 140 minutes contact with the materials. Values for untreated materials are calculated as an average of rate constants of uptake when in light and dark conditions; values for porphyrin-incorporated materials are obtained from the sample kept in the dark

	Rate of ADPA uptake (s^{-1})	
	Untreated material	**Porphyrin-incorporated material**
0MMA	$2.0 \times 10^{-3} \pm 1.41 \times 10^{-4}$	$2.40 \times 10^{-5} \pm 1.79 \times 10^{-5}$
5MMA	$9.01 \times 10^{-4} \pm 8.03 \times 10^{-5}$	$1.24 \times 10^{-5} \pm 7.69 \pm 10^{-6}$
10MMA	$3.83 \times 10^{-3} \pm 1.41 \times 10^{-4}$	$8.80 \times 10^{-6} \pm 7.42 \times 10^{-6}$
15MMA	$9.12 \times 10^{-4} \pm 2.84 \times 10^{-4}$	$2.60 \times 10^{-4} \pm 4.48 \times 10^{-5}$

Table 5. Rate constants of photobleaching for each irradiated porphyrin-incorporated material after correction for ADPA uptake by subtraction of the rate constant from porphyrin-incorporated materials kept in the dark.

	Rate constant, k (s^{-1})
0MAA	$4.64 \times 10^{-3} \pm 1.94 \times 10^{-4}$
10MAA	$3.09 \times 10^{-3} \pm 1.48 \times 10^{-4}$
20MAA	$3.48 \times 10^{-3} \pm 1.14 \times 10^{-4}$
30MAA	$5.76 \times 10^{-3} \pm 4.28 \times 10^{-4}$
0MMA	$3.08 \times 10^{-3} \pm 1.22 \times 10^{-4}$
5MMA	$3.09 \times 10^{-3} \pm 1.48 \times 10^{-4}$
10MMA	$1.87 \times 10^{-3} \pm 3.06 \times 10^{-4}$
15MMA	$6.34 \times 10^{-3} \pm 4.09 \times 10^{-4}$